Journal of Metals, Materials and Minerals, 35(1), e2195, 2025

Structural and dynamic analysis of tapered mast bladeless wind turbines using FEA and CFD for renewable energy generation

A. PRADEEP[1,*], Raman KUMAR[2,3], P. S. SATHEESH KUMAR[4], Nagaraj PATIL[5], Vijayakumar SIVASUNDAR[6,7], P. VIJAYA KUMAR[8], Selvaraj MANICKAM[9], Debasish SHIT[10]

[1] *Department of Mechanical Engineering, Saveetha School of Engineering, SIMATS, Chennai, Tamilnadu, India*
[2] *University School of Mechanical Engineering, Rayat Bahra University, Kharar, Punjab 140103, India*
[3] *Faculty of Engineering, Sohar University, PO Box 44, Sohar, PCI 311, Oman*
[4] *Department of Physics, NPR College of Engineering and Technology, Natham, Dindigul - 624 401, Tamilnadu, India*
[5] *Department of Mechanical Engineering, School of Engineering and Technology, JAIN (Deemed to be University), Bangalore, Karnataka, India*
[6] *Department of Mechanical Engineering, Graphic Era Hill University, Dehradun-248002, Uttarakhand, India*
[7] *Department of Mechanical Engineering, Graphic Era Deemed to be University, Dehradun-248002, Uttarakhand, India*
[8] *Department of Mechanical Engineering, Raghu Engineering College, Visakhapatnam, Andhra Pradesh-531162, India*
[9] *Department of Automation and Robotics, IMPACT College of Engineering and Applied Sciences, Bangalore*
[10] *Centre for Research Impact & Outcome, Chitkara University Institute of Engineering and Technology, Chitkara University, Rajpura, 140401, Punjab, India*

***Corresponding author e-mail**: drapradeep.mech@gmail.com

Received date:
5 November 2024
Revised date:
11 December 2024
Accepted date:
10 January 2025

Keywords:
Tapered mast;
Vortex shedding;
CFD analysis and structural deformation

Abstract

The present analysis investigates the possibility of using a tapered mast profile for bladeless wind turbines (BWTs) to enhance the function of extracting wind energy through the phenomenon of vortex-induced vibrations. Conventional HAWTs which remain the most efficient are however, costly in maintenance, mechanically complicated and rather unfavourable to the environment. To overcome these challenges a prototype BWT with a 0.6 m tapered mast was developed for the currents using mild steel and hollow square steel sections. Wind tunnels were also used to compare stress distribution, structural deformation and vane vortex shedding for the building at different wind speeds. The maximum calculated equivalent stress on the mast was 1.63×10^5 Pa with the total deformation achieving 1.732×10^{-6} m at a wind speed of 4 m·s^{-1}. The tests have represented an independent check on mast dynamics using recorded wind at an average of 7 m·s^{-1} and have quantified the observed oscillations marking validity of the dynamic behavior observed through simulations. Piezoelectric sensors deployed to measure mechanical stress produced voltage responses of 7.68 mV, 28.865 mV and 44.915 mV at wind velocities of 5.5 m·s^{-1}, 6.1 m·s^{-1} and 7.8 m·s^{-1} respectively. Findings show that wave amplitude of the oscillations increases with wind velocity and concomitantly voltage generated. The study highlights the potential of tapered mast geometries in improving structural efficiency and energy output.

1. Introduction

Recently, the options possible in the field of Renewable Energy (RE) source have dramatically improved, and a vast selection of converting the renewable resources into usable energy has availed itself, such as sunlight, air, sea waves, tides, and geothermal heat [1]. This development in renewable energy resources has been because of awareness of environmental and economic implications of the decline in fossil energy sources globally, rising cost of fuel and conventional electric power [2]. Significantly there has been improvement in the availability of actual or new RE resources with reliability and cost factors becoming more stable. Of these sources, wind energy stands out as the most sustainable, and conventional wind turbines have been the primary means of vegetation for tapping this energy [3]. However, the primitive wind turbines need a big space to be installed and cover vast area which is a demerit in some ways. These challenges have however attracted significant interest in a novel technology referred to as the vortex induced bladeless wind turbine. Pelamis OWT technology is totally different from the traditional blades and expensive plot of ground, which provides the service of better use of space. This makes it easy to place it most preferably within compact areas such as within residential buildings and commercial buildings, along roadsides where space is limited.

The need to make efficient use of renewable energy resources has made introduction of efficient wind turbine structures. Conventional wind turbines, particularly those of horizontal axis type (HAWT) have been the most widespread technology in wind power systems. However, questions were raised as to the effect of these devices on the environment, their mechanical site and cost of maintaining such innovation have led to research for new technologies [4]. Bladeless

wind turbines (BWTs) have recently emerged as a convenient option due to possible advantages as compared to traditional ones, including diminished mechanical stress and lower service prices [5]. Research conducted to compare the efficiency of BWTs to HAWTs has given different results. For instance, current theoretical studies indicate that fixed speed bladeless turbines are estimated to be about 30% less efficient than bladed turbines because of the differences in the mechanics of the two turbines [6]. On the other hand, other studies point out that BWTs can generate power at low energy levels, and the energy levels that they generate can be 50% to 70% of that of the solar panels per metre square at its best [7]. Recent work also notes the need to advance bladeless mechanisms of power generation so that the average efficiency of contemporary bladeless designs reaching 2% By steady state [8].

The increase in the rate of using renewable energy source has led to the technological development in designing wind turbines with enhanced efficiency, reduced cost, and minimal negative effects on the environment [9,10]. The mature technology of the horizontal-axis wind turbines or HAWT has been ruling the global wind energy market as these are highly reliable and efficient [11,12]. However, due to size, noise, maintenance, and effect on bird life their large mechanical systems motivated research for new technologies [13-15]. Of all these innovations, the bladeless wind turbines (BWT) have presented themselves as one of the most viable due to aerodynamics and mechanical systems [16]. VIV based blade less turbines have certain advantages including an expected lower maintenance cost and reduced environmental impacts [17,18]. As it is to be noted that the BWT does not possess such constituents of turbines like rotating blades and gearboxes; therefore, it contains lesser parts and has causes least mechanical abrasion [19,20].

The above-stated design advantages have made bladeless turbines especially appropriate for use in city-centre zones and low wind areas [21]. However, the present research shows that BWTs are less efficient than HAWTs; in similar conditions, they can produce roughly a third less output [22,23]. In contrast, the authors claim that there are specific characteristics of bladeless turbines that can help them achieve performance level necessary to make up for their inefficiency. For instance, they can occupy less floor area, they can perform effectively even at low wind speeds, and they are less noisy [24-26]. Moreover, some analyses have also shown that bladeless turbines can also produce almost the same density of energy as the photovoltaic panels, when both are put under the best use [27]. However, current work in design optimization and power generation mechanisms that distinguish bladeless turbines from their counterparts still require exhaustive improvement to realize their full potential [28].

In the past, more systematic HAWTs that are widely researched in terms of performance, efficiency, etc., suffer from mechanical complexity, maintenance prerequisites and environmental concerns. Contrarily, bladeless wind turbines (BWTs) can be seen a prospect option as they are capable to extract wind energy using vortex-induced vibrations. However, to date, little attention has been paid to mast geometries other than standard mast configurations, for instance the cylindrical mast, and little investigation has been done on the structural and aerodynamic response of tapered mast style under dynamic wind loads. In addition, the extensive area of mixing, swirling, and multiple connections between vertical and laterally tapered channels and their corresponding forces and energy distributions is still largely uncharted. This research seeks to fill these gaps by evaluating the structural response, stress distribution and aerodynamic viability of the proposed short tapered mast design through calculations of CFD and FEA and Experimental Tests. This paper also has a research intent to quantify the structural health, structural dynamics and firm power response characteristics of the bladeless wind turbines utilizing piezoelectric sensors for energy applications. Finally, the study helps progress the knowledge of tapered mast geometries imposed on the vortex shedding dynamics and the improvement of energy production potential of the bladeless wind energy system.

2. Materials and method

When selecting the components for the mast and base construction, two primary factors were considered: which are cost efficiency and easy to use. In the experimental investigation, metal sheets of mild steel and square steel hollow sections were employed. Design, fabrication, and analysis constitute three main aspects of the experimental method being used in the study. The first phase involves conducting a critically analytical review of what is already known in the academe about the wind responses and structural characteristics of tapered masts and the dynamic motion of structures in this maze. In the phase two, material selection for prototype and assembly of the model is the major work. The third phase of the design utilises the FEA in modelling how the tapered mast would behave under varying wind conditions and examine the stress level and structural strength. Furthermore, CFD models are used to investigate the forces acting on masts as well as the influence of the latter on mast stability.

This methodology aims at ascertaining versatility and provides a broad understanding of how mast activity narrows down and contribute to the design evolution where structural efficiency of engineering application is concerned, they use numerical modelling and experimental and computational analysis. Actively, using airflow, into structures such as masts, piezoelectric sensors are installed to convert mechanical stress into electrical current. Bladeless wind turbines harness the energy from oscillations and vortices by use of wind, to produce electricity. In case wind blows against a rotating body such as conical or cylindrical structure, the phenomenon experienced is known as vortex shedding. Controlling these vortices and oscillating in response to wind, bladeless turbines can capture energy and converting oscillations into electric current. This new approach holds the possibility of creating long-term power from wind energy of the surrounding atmosphere.

2.1 Design

A mast – a usual shape of a vertical support – is usually a uniformly cylindrical piece. Current research yet again brought to light another form of deviation from this classical method- the use of a tapered mast design. This is not only enhancing the way mass is distributed on this structure, but also closely addresses the impact of periodic oscillation caused by wind forces. The layout of the tapered mast configuration is such that it is shaped in a hollow cylindrical structure, set apart by its measurements. This mast measures 0.6 m in height and has a diameter of 0.115 m at the crown with the diameter reducing to 0.065 m at the base. As stated, previous literature mast has a minimum

length of 0.9 m, this research investigates the effect and/or behaviour of a shorter mast length of 0.6 m. The schematic of bladeless wind turbine is extrapolated as follows in the Figure 1.

2.2 Fabrication

In the construction of the mast and base of the BWT, mild steel sheet metal was used as well as HSS square steel pipes. This choice gives stability and durability; something that is important in shaping this prototype. The HSS square steel pipes are easy to fit in within the production process and possess adequate strength to carry the structure. Choosing mild steel for mast, it was malleable, and easy to manipulate and bend in the way it was required. Its flexibility allowed for the easy rolling of the metal to the needed measurements for the structure of the mast. The base of this IOT prototype had a height of 1.2 m and had a length and breadth of 0.45 m. These dimensions were selected to enable the prototype to have rigid support that will fit its intended use. Six piezoelectric sensors were used where all the sensors were divided into three different groups, each containing two sensors. These sensor groups were located beneath a circular disc which was welded to the base of the mast. Sensors in each set were wired in series just to yield the greatest voltage the circuits can generate. Fig presents the experimental setup of the bladeless wind turbine and the details of the wound turbine are given in Table 1.

The nature of these measurements is to be semiquantitative and relative, but to make the tests as clear cut as possible, a stringently standardized procedure was adhered to throughout the experiments. To ensure that the results obtained were stable the prototype BWT was exposed to different wind conditions at regular time intervals for different consecutive days. The wind speed data was collected from three positions (10:00 AM, 11:00 AM and 12:00 PM) to capture natural fluctuation of wind flow. To minimize random errors, each experimental trial was done thrice and the mean voltage obtained were used for further analysis. To eliminate vibrations different from those produced by the wind, the setup we used was mounted on a stable platform (the roof of a 3-story building). Additionally, the multimeter used to record voltage output was standardized before use, and Networks® piezoelectric sensors were checked for connectivity to ensure there was no signal interruption. It also helped in capturing actual response including structural and dynamic features of the mast.

2.3 Analyses

In the 2D analysis, our interest lies in studying the Von Karman vortices behind the cylindrical mast with a top layer diameter of 11.5 cm. The mast was considered as being smooth and homogeneous for modelling purposes to keep important features intact while ignoring complicating factors that might have made computational analysis more difficult. A detailed 2D scan of this top layer forms part of further aerodynamic characterization and determination of lift forces using computational simulations. An additional boundary layer was set around the cylinders to capture the boundary layer effects around the cylinder surface accurately as depicted in the Figure 2(a). The numeric for the present cases have been done with ANSYS FLUENT and LES as the viscous model has been used since it is effective in capturing unsteady flows. Thus, the present study offers time history of turbulent flow and demonstrates instantaneous flow oscillations and vortex shedding frequency as well as the pattern of shedding over time. The dimension of fluid domain and boundary conditions for the setup is clearly illustrated in the Table 2-3. While comparing the peak values of the drag coefficient (Cd), and the lift coefficient (Cl), different waves forms can be observed signifying the formation of a vortex. The visualization of vortex pattern can be seen in Figure 2(b). These patterns, which look like sinusoidal wave forms, start to become most apparent after the 15 th second and may indicate that there is a transition in the flow dynamics around the structure.

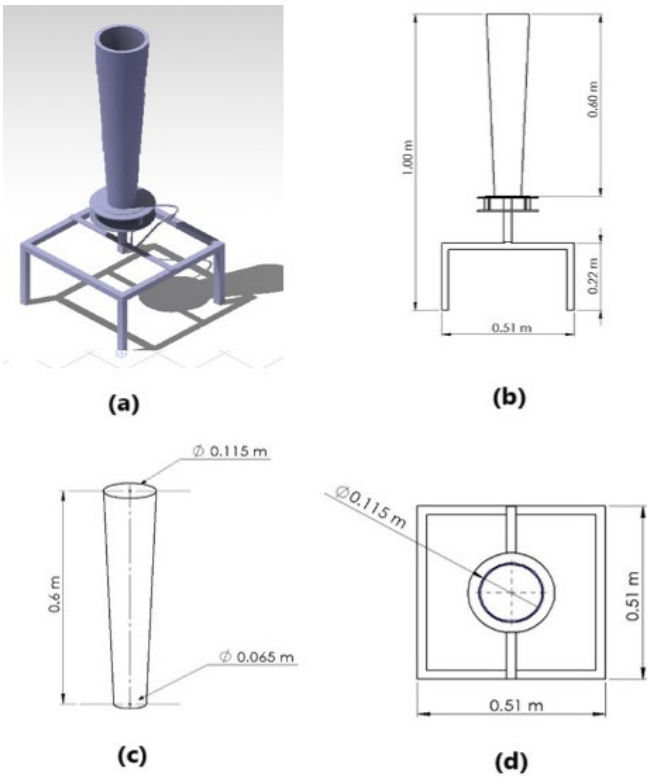

Figure 1. BWT (a) Schematic diagram, (b) Side view, (c) Mast, and (d) Top view.

Table 1. Dimensions of the prototype.

Parameters	Values
Total length	0.45 m
Total breadth	0.45 m
Total height	1.25 m
Total weight	5.5 Kg
Mast weight	1.5 Kg
Mast height	0.6 m
Bottom diameter of the mast	0.065 m
Top diameter of the mast	0.115 m
Mast tapper angle	2.4°

Table 2. Dimension of fluid domain.

Parameter	Dimension
D1	115 mm
H1	4000 mm
V1	2500 mm

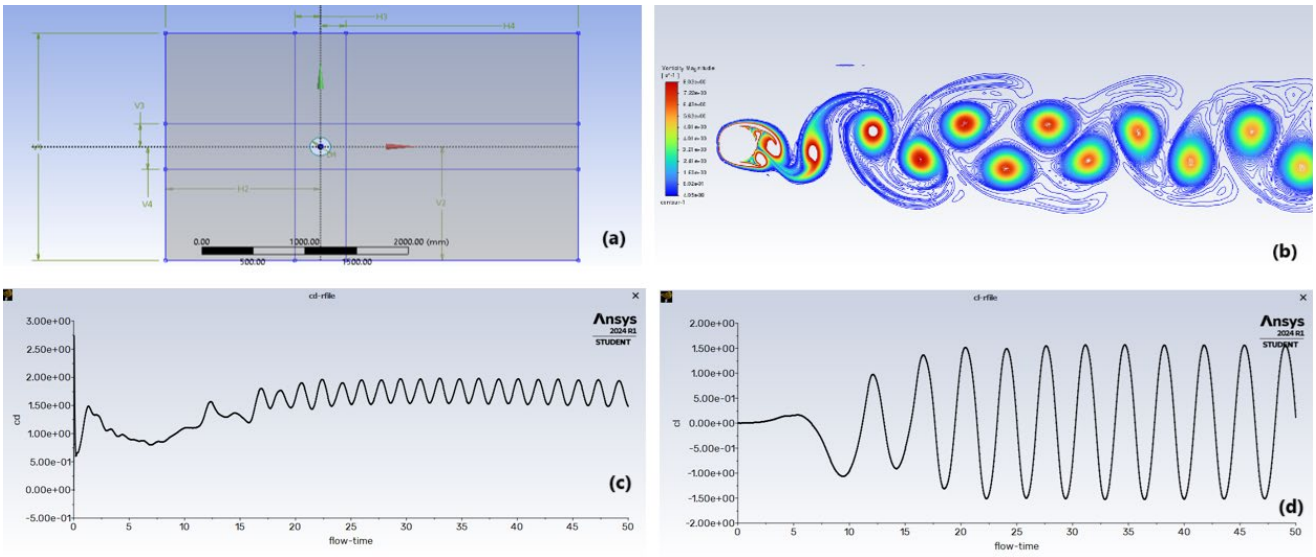

Figure 2. (a) Geometry of fluid domain, (b) Visualization of vortex patterns, (c) Drag co-efficient vs time graph, and (d) Lift co-efficient vs time graph.

Table 3. Boundary conditions for the set up.

Boundary conditions	Values
Material state	Fluid
Fluid type	Air
Inlet velocity	0.08 $m \cdot s^{-1}$
Outlet pressure	0 Pa
Reference area	0.06 m^2
Viscosity	0.0000178 $Kg \cdot m^{-1} \cdot s^{-1}$)

The appearance of vortices, associated with these characteristic waveforms, indicates that there are combined interactions of forces in the field of the flow. In the Figure 2(c-d), Besides that, the regular fluctuations represented in the graph are associated with the active movement of the fluid when interacting with the structure. such variation depicts the stagered oscillation in force acting on the cylinder, where forces or its magnitude show periodicity in their variation. It means that around the cylinder, there are force's positive and negative values, which appear in a cycle progress force distribution. These push and pull forces applied on the cylinder causes oscillation like reactions in the motion of the cylinder. The force magnitudes vary periodically as the fluid passes through the structure and the cylinder responds in a dynamic fashion as it moves in a cyclic fashion to and fro. Therefore, the oscillations demonstrated in the graphs provide a clear correspondence between the temporal variation in the force distribution process and the cyclical changes in structural response or interaction influenced by the fluid flow. In this study, the 3D analysis provides a full understanding of the fluid flow patterns developed around the mast structure distribution. These alternating forces exerted on the cylinder induce corresponding oscillations in its motion. As the fluid flows around the structure, the periodic variation in force magnitudes drives the cylinder to oscillate, resulting in a dynamic response characterized by rhythmic movement. Thus, the observed oscillations in the graphs directly correlate with the cyclic nature of force distribution and subsequent structural response induced by the fluid flow dynamics.

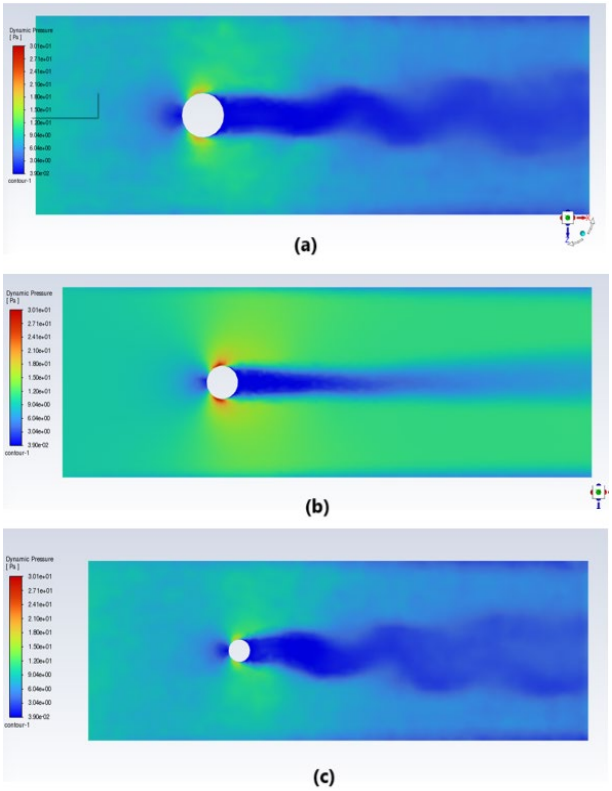

Figure 3. Pressure contour (a) at the top surface of the mast, (b) at the middle surface of the mast, and (c) at the bottom surface of the mast.

The 3D analysis conducted in this study enables the examination of the fluid flow patterns around the mast structure comprehensively. From the CFD simulations, the flow pattern at different layers of the mast which had been positioned in the crosswise fashion with respect to the longitudinal axis of the mast can be analyzed. As will be seen soon these layers were mounted at different heights within the mast – the top, middle and at the base section – and this allowed the investigators to observe how the fluid engages with the mast along

its height. With the aid of flow visualization at these different layers, insights is obtained into the distribution of the aerodynamic loads and pressures on the mast. The pressure contour for mast at all surfaces is shown from the Figure 3. The analysis enables us to realize the parts of the possibility of a turbulent, separate, or re circulation, which hugely affects the structural sturdiness and productivity of the mast. Moreover, analyzing the flow characteristics in several layers allows us to assess the impact of mast geometry – tapering, for instance – by observing the resulting flow patterns and loads acting upon the structure. This information was very valuable in determining the best design for the mast in order to reduce the drag forces on the structure. The pathlines with the velocity of forces on the surfaces of mast can be clearly seen from Figure 4. Visualization of flow of particles can be seen around and behind the mast in the Figure 5.

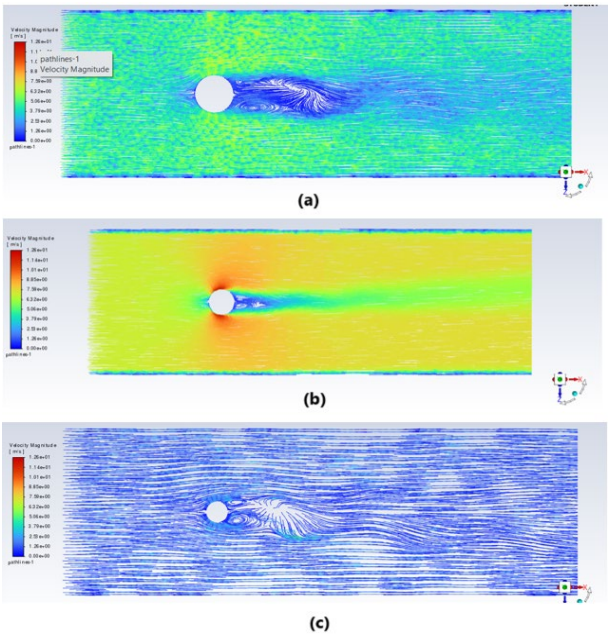

Figure 4. Velocity path lines (a) at the top surface of the mast, (b) at middle surface of the mast, and (c) at the bottom surface of the mast.

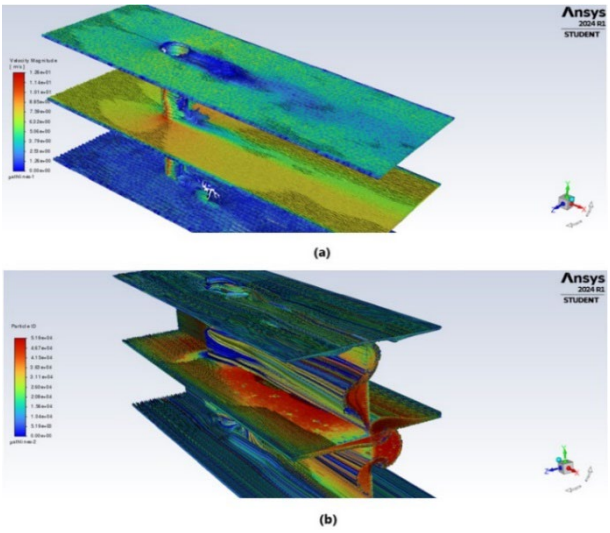

Figure 5. Visualization of flow pattern (a) around the mast (b) behind the mast.

3. Results and discussion

In order to provide a frame of reference for the performance of the tapered mast BWT, a comparison was made with benchmark small-scale Horizontal Axis Wind Turbines (HAWTs). It will be realized that a 10 W rated small scale HAWT may produce voltage in the order of 100 mV to 150 mV with wind speeds of 6 $m \cdot s^{-1}$ to 8 $m \cdot s^{-1}$. A comparison has been made with this study BWT tapered mast which at wind speed of 5.5 $m \cdot s^{-1}$, 6.1 $m \cdot s^{-1}$ and 7.8 $m \cdot s^{-1}$ delivered 7.68 mV, 28.865 mV and 44.915 mV voltage output respectively. Despite lower output voltage, the BWT has advantageous characteristics such as less complex structure, lower price, and fewer demands for maintenance compared to the conventional HAWT. The trade-off is in the conversion efficiency of the energy in which further enhancement can be attained through the better material selection of piezoelectric material, the particular mode of arrangement of the piezoelectric layer and the mast geometry. The outcome further suggests that bladeless turbines, despite being a relatively novel technology at the moment, could represent a strong development in achieving an inexhaustible generation in low-wind environments and cities that would not allow for HAWTs installation.

The structural analysis proved to be an essential element in making conclusions regarding the state of a structure when exposed to various forces and pressure it might face. In particular, the total deformation of the mast and the distribution of Von Mises stress is determined more thoroughly in this analysis with reference to the ANSYS Workbench static structural module as seen in Figure 6. When geometric details of the mast are scaled and numerically modeled, extensive information on structural response under different loading is obtained by simulation alone. The maximum equivalent stress which is acting on the mast is estimated as 1.63×10^5 Pa, the total deformation of the mast is estimated after applying the wind parameter to be 1.732×10^{-6} m for wind speed $u = 4$ $m \cdot s^{-1}$. The deformation of the mast can be identified in Figure 7.

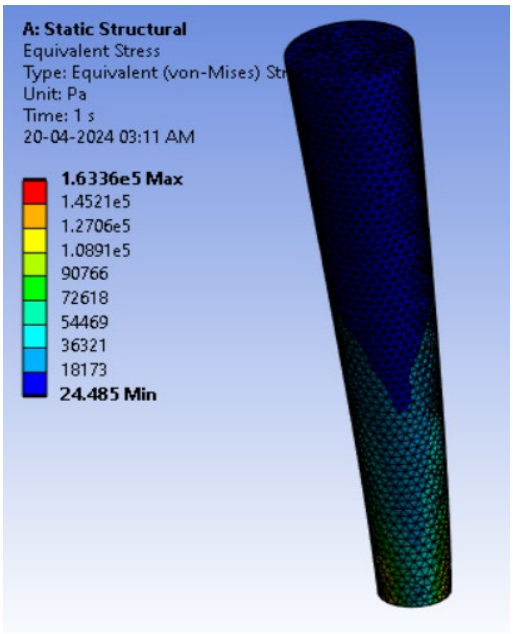

Figure 6. Equivalent stress analysis on mast.

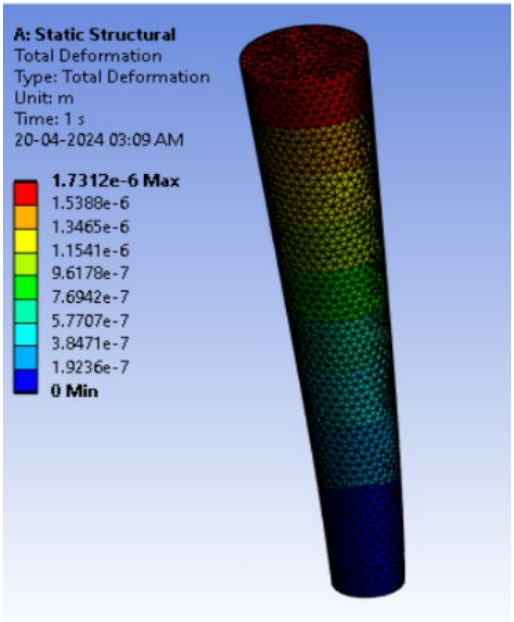

Figure 7. Total deformation of the mast.

3.1 Design calculations

Reynolds number is a non-dimensional measure which is described in fluids dynamics to identify a style of flow of a fluid about an item. In particular regarding vortices, the Reynolds number was used to identify if the flow was laminar or turbulent [32,33]. It was found out as the ratio of Inertia forces to Viscous forces along with the fluid. When looked at vortices, the Reynolds number helps in determining the stability of such rotating fluid areas within the circulation movement.

$$\text{Reynolds number, Re} = \frac{\rho \times U \times L}{\mu} \quad (1)$$

$$= \frac{1.225 \times 0.08 \times 0.2}{0.0000789}$$

$$= 1094.98$$

$$\approx 1095$$

Where:

P = the density of the fluid ($Kg \cdot m^{-3}$)

U = the characteristic velocity of the flow (velocity magnitude) ($m \cdot s^{-1}$)

L = characteristic length scale of the flow (diameter of a cylinder, characteristic length of the object) (m)

μ = the dynamic viscosity of the fluid ($Kg \cdot m^{-1} \cdot s^{-1}$)

The Strouhal number (St)was another dimensionless parameter employed in fluid mechanics; especially with reference to flow past bluff bodies, to describe the periodic shedding of vortices. The Strouhal number was defined as the ratio of the frequency of vortex shedding (f) to the product of the flow velocity (V) and a characteristic length scale (L) of the object The Strouhal number St was defined as the ratio of the frequency of vortex shedding (f) to the product of the flow velocity (V) and a characteristic length scale (L) of the object.

$$\text{St} = \frac{f \times L}{U} \quad (2)$$

Where:

f = frequency of vortex shedding (in Hz or cycles per second),

U= the characteristic velocity of the flow .

L = a characteristic length scale of the object (diameter of a cylinder)

St when 250<Re<1200

At Re 1095,

$$\text{St(theroritical)} = 0.2129 \quad (3)$$

$$\text{St(analytical)} = \frac{f\,(analytical) \times L}{U} \quad (4)$$

(Since L = D)

$$= \frac{0.0913 \times 0.2}{0.08}$$

$$= 0.2285$$

$$\text{f(theoretical)} = \frac{St(theoretical) \times U}{d} \quad (5)$$

$$= \frac{0.2129 \times 0.08}{0.2}$$

$$= 0.08516$$

$$\text{f(analytical)} = 0.0913$$

3.2 Environmental conditions

In the experimental trial, the prototype bladeless wind turbine was mounted on the roof of a three story building where it was oriented to the prevailing wind conditions. Having an average wind speed of about 7 $m \cdot s^{-1}$, the environmental conditions of the site caught some real world situations and therefore testing the efficacy of the prototype in such a natural environment well suited the purpose. However, thanks to the moderate wind speed the movement of the mast was recognized as oscillating which proves the dynamic behaviour of the structure subjected to the wind loads. While these oscillations seemed to be relatively small in angle the researchers stressed that it was important in light of the fact that the mast has weight and therefore puts pressure on the disc. This force, while being subliminal, was effectively measured by the piezoelectric sensors that were placed within the structure, which was designed work as a mechanical stress and pressure gauge [34-36].

Because force has to be discussed in a very quantified manner, a comprehensive force measuring protocol was used. The positive and negative aspects of the piezoelectric circuit were manually wired to a high accuracy digital multimeter with necessary pre-setting to measure the voltage and amperage changes accurately. Real-time monitoring of the response of the structure was achieved through this device, which offered detailed information on the structural performance of the mast under loads from the wind thus giving detailed information of the performance of the mast in different natural conditions. Mean wind velocity of 5.5 $m \cdot s^{-1}$ in the analysis was identified an average voltage of 7.68 mV at first reference hour as depicted in Figure 8(a).

This implies that as the wind speed the force experienced by the mast due to wind also increases Successively. As a result, the amount of force on the piezoelectric sensors vary to and fro within one second and vice versa, the voltage readings are reciprocated in the very same manner.

Graph shown in Figure 8(b) represents the voltage-time curve corresponding to the second reference hours but with a wind speed of 6.1 m·s^{-1}. In this case, mean was calculated as 0.028865 V. As seen from the graph, the more the wind speed rises, the force on the mast is also going up and so influencing the voltage depicted by piezoelectric for different sails. This dynamic relationship clearly shows how velocity of wind determines voltage and how sensitive the system is to these environmental changes. The voltage-time plot depicted in Figure 8(c) is obtained for similar reference hours but in this case wind speed of 7.8 m·s^{-1}. At this increased wind velocity, the average voltage recorded was 44.915 mV. As before, the graph shows how the force due to the wind on the mast translates with proportionality to the force that the piezoelectric sensors are experiencing, resulting in oscillations of the voltage output in real-time. The following are the voltage in relation to the time recorded by a multimeter for three different reference time like 10:00 AM, 11:00 AM and 12:00 PM respectively. Such graphs are useful in understanding fluctuations that occur in voltage output with respect to the wind speed, and as such represent the performance of the system given different environmental factors.

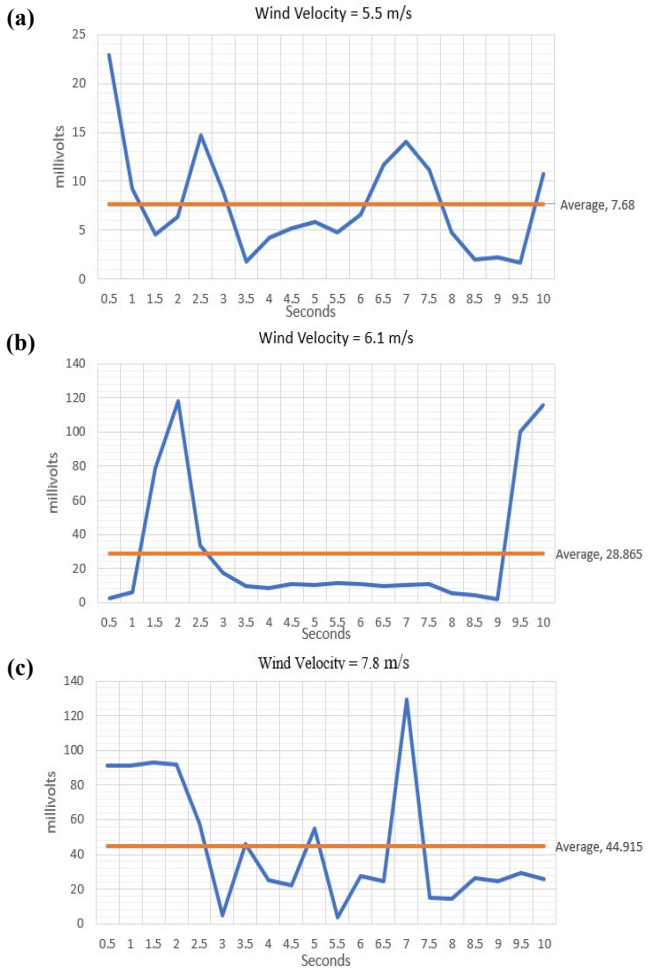

Figure 8. Readings from (a) first reference hour, (b) second reference hour, and (c) third reference hour.

Contained in the image are three-line graphs depicting voltage output (in mV) with time (in s) plotted on the vertical and horizontal axes respectively, measured at various wind velocities. For Graph (a), with thrust wind velocity of 5.5 m·s^{-1}, the voltage output has a small range of variation for the 10 s period, and the average voltage is 7.68 mV as shown in the Figure. At a higher wind velocity of 6.1 m·s^{-1} in Graph (b) a higher voltage is registered at the initial stage then the voltage output reduces and remains relatively steady, the average voltage recorded 28.865 mV. This means that besides the assumed fixed force in the direction of the wind on the central portion of the mast, a greater passing force due to elevated winds is exerted on the mast. In Graph (c), where the wind velocity is 7.8 m·s^{-1} the voltage output continues to demonstrate increased fluctuation with numerous peaks and troughs implying more complex dynamic wind-mast interactions. The mean voltage generated for this case is 44.915 mV as the graph increasingly shows the voltage generated with the increase in the wind speed. All in all, data obtained show that wind velocity directly correlates to the mechanical motion that powers the piezoelectric sensors due to enhanced energy transfer resulting in increased voltage generation as the velocity increases.

3.3 Practical energy harvesting implications of voltage output

Energy scavenging has evolved as an effective solution for the supply of power to self-contained electronics by extracting mechanical energy from the environment. TENGs have attracted much attention for their high output, flexibility and diversely potential applications in the areas of self-powered systems. New research advances in TENGs have been directed towards improving performance through new materials and geometry. For example, A modified TENG using 2D raw material graphene-related carbon nitride thin film has been claimed to enhance the efficiency for energy conversion for building self-powered systems [29]. In addition, others have examined the structure, working principle and the prospect of the TENGs in different energy conversion applications [30]. TENGs have also been incorporated into flexible and wearable energy harvesting systems by virtue of which they are suitable for use in wearable electronics and other flexible devices [31]. The voltage outputs recorded during the experimental trials the basic element for assessing the practical energy harvesting potential of the bladeless wind turbine (BWT). Therefore, the following discussion aims at identifying the relation of these voltage values to practical applications in power generation and efficiency of various energy harvesting systems.

The electrical energy harvested by piezoelectric sensors can be estimated using the basic power equation:

$$P = V^2 / R$$

Where: P = power output in watts, V = voltage generated by the sensors, R = Electrical load resistance. For this study, assuming a representative load resistance of 1 MΩ, the corresponding power outputs for different wind speeds can be calculated as follows:

At 5.5 m·s^{-1} wind speed (mean voltage = 7.68 mV):
$P = (7.68 \times 10^{-3})^2/10^6 = 5.9$ nW

At 6.1 m·s^{-1} wind speed (mean voltage = 28.865 mV):
$P = (28.865 \times 10^{-3})^2/10^6 = 833$ nW

At 7.8 m·s^{-1} wind speed (mean voltage = 44.915 mV):
$P = (44.915 \times 10^{-3})^2/10^6 = 2.02$ μW

From these findings there exists a strong correlation between the wind speed and the amount of energy captured. The current prototype offers small voltage and power outputs it apparent that the practical potential of energy harvesting using the device is shown in those power requirements that are low and where conventional wind turbines are not viable. The outcomes provide the further optimisation and scaling of the system and at the same time allows considering it as the viable solution for energy generation at the sustainable and decentralised level.

4. Conclusion

Overall, the results of the experimental study of the bladeless wind turbine model with a conical mast indicate the possibility of using vortex-induced oscillations for the effective capture of wind energy. The numerical computations and Computational fluid dynamics results proved that the tapering pattern refocused forces over the mast profile and thus minimized oscillations. When oscillating the mast with a mean wind speed of 5.5 m·s^{-1} the average voltage was 7.68 mV and when increasing the wind speed to 7.8 m·s^{-1}, the average was 44.915 mV. From the variation in voltage output over the reference time, the dynamic response of the mast to fluctuating wind conditions was demonstrated. Implications of these results show that apart from the initial and volume cost, low-frequency wind-induced oscillation can be harvested by the tapered mast structure for generating power, which can be useful for low-cost and bladeless wind energy application

References

[1] A. Mane, M. Kharade, P. Sonkambale, S. Tapase, and S. S. Kudte, “Design & analysis of vortex bladeless turbine with gyro e-generator,” *International Journal of Engineering Research and Technology*, vol. 3, pp. 445-452, 2017.

[2] I. Bahadur, “Dynamic modeling and investigation of a tunable vortex bladeless wind turbine,” *Energies*, vol. 15, no. 18, p. 6773, 2022.

[3] A. Bani Hani, “*Wind flow induced vibrations of tapered masts*,” M.S. thesis, Department of Civil Engineering, Cleveland State University, Cleveland, OH, USA, 2009.

[4] A. Smith, and B. Yu, “Wind energy technology: A review of efficiency and innovation,” *Journal of Renewable Energy Systems*, vol. 45, no. 2, pp. 213-225, 2020.

[5] C. Lopez, M. Pérez, and J. Torres, “A study on the mechanical efficiency of bladeless wind turbines,” *Applied Energy Research*, vol. 16, no. 4, pp. 309-320, 2019.

[6] J. Johnson, and S. Wang, “Comparative performance of bladeless and conventional wind turbines,” *International Journal of Wind Energy*, vol. 12, no. 3, pp. 145-158, 2021.

[7] M. Aranca, “Bladeless wind turbines: Efficiency analysis and applications,” *Energy Technologies Review*, vol. 7, no. 1, pp. 98-107, 2021.

[8] K. Zhou, and R. Yu, “Theoretical analysis of the bladeless wind turbine performance,” *Journal of Wind Energy Technology*, vol. 22, no. 5, pp. 331-342, 2018.

[9] A. D. Sahin, "Progress and recent trends in wind energy," *Progress in Energy and Combustion Science*, vol. 30, no. 5, pp. 501-543, 2004.

[10] M. Ragheb, and A. M. Ragheb, "Wind turbine gearbox technologies," in *Fundamental and Advanced Topics in Wind Power*, R. Carriveau, Ed. InTech, 2011, pp. 1-34.

[11] S. Eriksson, H. Bernhoff, and M. Leijon, "Evaluation of different turbine concepts for wind power," *Renewable and Sustainable Energy Reviews*, vol. 12, no. 5, pp. 1419-1434, 2008.

[12] J. F. Manwell, J. G. McGowan, and A. L. Rogers, *Wind Energy Explained: Theory, Design and Application*, 2nd ed. Wiley, 2009.

[13] T. Burton, D. Sharpe, N. Jenkins, and E. Bossanyi, *Wind Energy Handbook*, 2nd ed. Wiley, 2011.

[14] P. J. Schubel, and R. J. Crossley, "Wind turbine blade design," *Energies*, vol. 5, no. 9, pp. 3425-3449, 2012.

[15] R. Gasch, and J. Twele, Wind Power Plants: Fundamentals, Design, Construction and Operation, 2nd ed. Springer, 2012.

[16] M. S. Adaramola, "Wind turbine technology: Principles and design," in *Wind Turbine Technology: Principles and Design*, Apple Academic Press, 2014, pp. 1-30.

[17] S. Mathew, Wind Energy: Fundamentals, Resource Analysis and Economics. Springer, 2006.

[18] D. A. Spera, Wind Turbine Technology: Fundamental Concepts of Wind Turbine Engineering, 2nd ed. ASME Press, 2009.

[19] R. D. Prasad, and N. S. Boljanovic, "Wind turbine performance analysis using CFD," *International Journal of Energy and Environment*, vol. 4, no. 1, pp. 1-8, 2013.

[20] M. M. Hand, S. F. Baldwin, E. Demeo, J. M. Reilly, T. Mai, D. Arent, G. Porro, M. Meshek, and D. Sandor, "Renewable electricity futures study," *National Renewable Energy Laboratory (NREL)*, Golden, CO, USA, Technical Report, NREL/TP-6A20-52409, 2012.

[21] A. D. Hansen, P. Sørensen, F. Iov, and F. Blaabjerg, "Centralised power control of wind farm with doubly fed induction generators," *Renewable Energy*, vol. 31, no. 7, pp. 935-951, 2006.

[22] G. M. Joselin Herbert, S. Iniyan, E. Sreevalsan, and S. Rajapandian, "A review of wind energy technologies," *Renewable and Sustainable Energy Reviews*, vol. 11, no. 6, pp. 1117-1145, 2007.

[23] M. Z. Jacobson, and M. A. Delucchi, "A path to sustainable energy by 2030," *Scientific American*, vol. 301, no. 5, pp. 58-65, 2009.

[24] P. Moriarty, and D. R. Honnery, "What is the global potential for renewable energy?" *Renewable and Sustainable Energy Reviews*, vol. 16, no. 1, pp. 244-252, 2012.

[25] M. I. Blanco, “The economics of wind energy,” *Renewable and Sustainable Energy Reviews*, vol. 13, no. 16-17, pp. 1372-1382, 2009.

[26] M. L. Kubik, P. J. Coker, and C. Hunt, "The role of conventional generation in managing variability," *Energy Policy*, vol. 50, pp. 253-261, 2012.

[27] O. Ellabban, H. Abu-Rub, and F. Blaabjerg, "Renewable energy resources: Current status, future prospects and their enabling technology," *Renewable and Sustainable Energy Reviews*, vol. 39, pp. 748-764, 2014.

[28] T. L. Ruwa, S. Abbasoğlu, and E. Akün, "Energy and exergy analysis of biogas-powered power plant from anaerobic co-digestion of food and animal waste," *Processes (Basel),* vol. 10, no. 5, p. 871, 2022.

[29] K. Ruthvik, A. Babu, P. Supraja, M. Navaneeth, V. Mahesh, K. U. Kumar, R. R. Kumar, B. M. Rao, D. Haranath, and K. Prakash, "High-performance triboelectric nanogenerator based on 2D graphitic carbon nitride for self-powered electronic devices," *Materials Letters,* vol. 350, p. 134947, 2023.

[30] W.-G. Kim, D.-W. Kim, I.-W. Tcho, J.-K. Kim, M.-S. Kim, and Y.-K. Choi, "Triboelectric nanogenerator: Structure, mechanism, and applications," *ACS Nano*, vol. 15, no. 1, p. 258-287, 2021.

[31] M. He, W. Du, Y. Feng, S. Li, W. Wang, X. Zhang, A. Yi, L. Wan, and J. Zhai, "Flexible and stretchable triboelectric nanogenerator fabric for biomechanical energy harvesting and self-powered dual-mode human motion monitoring," *Nano Energy*, vol. 86, no. 106058, p. 106058, 2021.

[32] R. Alkarsifi, J. Ackermann, and O. Margeat, "Hole transport layers in organic solar cells: A review," *Journal of Metals, Materials and Minerals*, vol. 32, no. 4, pp. 1-22, 2022.

[33] A. Pandey, A. K. Upadhyay, and K. K. Shukla, "Lightning strike response of composite structures: A review," *Journal of Metals, Materials and Minerals*, vol. 31, no. 1, 2021.

[34] A. R. Wimada, N. P. D. Nitamiwati, F. T. Pratiwi, M. D. Solikhah, B. R. Barus, E. D. Wijanarko, R. Anggarani, L. Asiyah, S. Widodo, A. Thahar, and S. S. Wirawan, "SBR elastomer response to renewable diesel blends: An experimental investigation," *Journal of Metals, Materials and Minerals*, vol. 34, no. 4, e2020, 2024.

[35] S. Vijayakumar, N. Dhasarathan, P. Devabalan, and C. Jehan, "Advancement and design of robotic manipulator control structures on cyber physical production system," *Journal of Computational and Theoretical Nanoscience*, vol. 16, no. 2, pp. 659-663, 2019.

[36] P. Sharma, P. Paramasivam, B. J. Bora, and V. Sivasundar, "Application of nanomaterials for emission reduction from diesel engines powered with waste cooking oil biodiesel," *International Journal of Low-Carbon Technologies*, vol. 18, pp. 795-801, 2023.